Noise Leakage Suppression in FRF Measurements Using Periodic Signals

R. Pintelon, K. Barbé, G. Vandersteen, and J. Schoukens

Vrije Universiteit Brussel, dept. ELEC, Pleinlaan 2, 1050 Brussel, Belgium

Tel. (+32-2) 629.29.44, Fax. (+32-2) 629.28.50, E-mail: Rik.Pintelon@vub.ac.be

Abstract—The steady state response of a system to a periodic input is still corrupted by noise transients. For lightly damped systems these noise transients increase considerably the variance of the measured frequency response function (FRF). This paper presents a method that suppresses the influence of the noise transients (leakage errors) in FRF measurements. The method is based on a local polynomial approximation of the noise leakage errors on the FRF. Compared with the classical approaches, the proposed procedure is more robust and needs less measurement time. The theory is supported by a real measurement example[1].

I. INTRODUCTION

Frequency response functions (FRF) give a lot of insight in the dynamic behaviour of a system. They are measured by standard commercially available dynamic signal analyzers and network analyzers, and are used in all kinds of engineering disciplines for analysis, modeling, design, and protoyping [1], [2], [3]. Since the noise variance is used to calculate uncertainty bounds on the FRF with a given confidence level [3], [4], [5], a good estimate of the variance of the FRF is as important as the FRF value itself.

A first basic choice to be made when measuring the FRF concerns the nature of the excitation signal: arbitrary ([1], [2], [6], [7]) or periodic ([3], [4], [5], [8]). The advantages of using arbitrary excitations are the higher frequency resolution, the fact that operational data can be handled, and the simple experimental set up (no synchronisation between the generator and the acquisition unit is required). The disadvantages are the random magnitude of the DFT spectrum, and the need of a reference signal for solving the errors-in-variables problem (the input and the output observations are noisy). Periodic excitations have the following advantages [3]: the magnitude of the DFT spectrum can be imposed exactly, and suppression of the system transient (leakage) errors. Their disadvantages are the smaller frequency resolution and the more complicated experimental set up (exact synchronisation between the generator and the acquisition units is needed). This paper handles the periodic case for single-input, single-output systems.

Although the steady state response of a dynamic system to a periodic input is not subject to system transients, it is still corrupted by the noise transients. For lightly damped systems these noise transients (leakage errors) can increase considerably the variance of the FRF measurement. In this

paper we present a method for suppressing the noise transients (leakage errors) in nonparametric FRF measurements. The method assumes that the noise leakage (transient) errors on the FRF can locally be approximated by a polynomial of degree R. The main difference with the local polynomial approach for random excitations ([6], [9]) is that no local polynomial approximation of the FRF is needed by exploiting the periodic nature of the excitation. Via an in depth theoretical comparison with the classical methods [8], [10] it is shown in this paper that the proposed local polynomial approach reduces (i) the variance of the FRF measurement, (ii) the experimental time. These reductions are significant for lightly damped systems.

II. LINEAR SYSTEMS EXCITED BY A PERIODIC SIGNAL

A. Measurement setup

Fig. 1 shows a general setup for measuring the FRF of a linear time invariant (LTI) system using a periodic excitation. The LTI system can be measured in open (black lines) or closed (black and gray lines) loop, and the actuator and controller may behave nonlinearly. P periods of N samples each of the input and output are measured under steady state conditions. Hence, the measured input-output discrete Fourier transform (DFT) spectra of the pth period are given by

$$
\begin{aligned}
X^{[p]}(k) &= X_0(k) + N_X^{[p]}(k) \\
X(k) &= \frac{1}{\sqrt{N}} \sum_{t=0}^{N-1} x(t) e^{-j\frac{2\pi kt}{N}}
\end{aligned}
\tag{1}
$$

with $p = 1, \ldots, P$; $X(k)$, $X = U, Y$, the DFT spectrum of $x(t)$, $x = u, y$; $Y_0(k) = G(\Omega_k) U_0(k)$, $U_0(k)$ the DFT spectrum of the periodic part of the actual input of the LTI system; $G(\Omega_k)$ the true FRF of the LTI system; and $N_U^{[p]}(k)$, $N_Y^{[p]}(k)$ the input-output errors depending on the generator, the controller, and the process noise sources, and respectively the input and output measurement errors [3]. The generalized frequency variable Ω_k equals $j\omega_k$ for continuous-time systems ($\Omega = s$), and $e^{-j\omega_k T_s}$ for discrete-time systems ($\Omega = z^{-1}$), where $\omega_k = \frac{2\pi k f_s}{N}$ with $f_s = 1/T_s$ the sampling frequency. Modeling the input-output errors as filtered discrete-time or band-limited continuous-time white noise, the DFT spectra $N_U^{[p]}(k)$ and $N_Y^{[p]}(k)$ can be written as

$$
N_X^{[p]}(k) = H_X(\Omega_k) E_X^{[p]}(k) + T_{H_X}^{[p]}(\Omega_k)
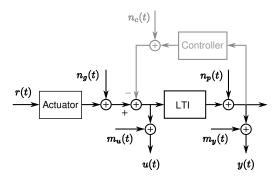\tag{2}
$$

Figure 1. Measurement of the FRF of an LTI system in an open (black) or closed (black and gray) loop setup. $r(t)$: signal stored in the arbitrary waveform generator; $n_g(t)$, $n_c(t)$, $n_p(t)$, $m_u(t)$, and $m_y(t)$: respectively the generator, the controller, the process, and the input-output measurement noise sources. The actuator and the controller may behave nonlinearly.

where $H_X(\Omega)$, $X = U, Y$, is a rational function of Ω representing the noise dynamics, $E_X^{[p]}(k)$ is the DFT of the unobserved (band-limited) white noise source $\left(\text{var}\left(E_X^{[p]}(k)\right) = O\left(N^0\right)\right)$, and $T_X^{[p]}(\Omega)$ is a rational function of Ω representing the leakage (transient) error of the DFT [3]. The latter decreases to zero as an $O\left(N^{-1/2}\right)$, increases the variance of the measured DFT spectrum, and introduces a correlation of the input-output noise over the signal period p.

The DTF (1) is scaled by $\sqrt{N}$ such that the variance of the frequency domain noise is an $O\left(N^0\right)$, which simplifies the bias analysis of the estimated noise (co-)variances. Afterward, to obtain an estimate of the Fourier coefficients, the DFT spectra are divided by $\sqrt{N}$. The latter are independent of the number of periods P and the number of samples N in the DFT, which simplifies the comparison over the different methods.

B. Nonparametric modeling - the classical method

The classical approach [3], [10] calculates the sample mean and sample (co-)variances over $P \geqslant 6$ DFT spectra (1)

$$\hat{X}_{\text{rect}}(k) = \frac{1}{P}\sum_{p=1}^{P} X^{[p]}(k)$$

$$\hat{\sigma}^2_{XL,\text{rect}}(k) = \frac{1}{(P-1)}\sum_{p=1}^{P} r_X^{[p]}(k)\overline{r_L^{[p]}(k)}$$

$$r_X^{[p]}(k) = X^{[p]}(k) - \hat{X}_{\text{rect}}(k) \qquad (3)$$

with, $\overline{x}$ the complex conjugate of x, $\hat{\sigma}^2_{XX}(k) = \hat{\sigma}^2_X(k)$, and $X, L \in \{U, Y\}$. The expected values of the sample means and the sample (co-)variances equal

$$E\left\{\hat{X}_{\text{rect}}(k)\right\} = X_0(k) \qquad (4)$$

$$E\left\{\hat{\sigma}^2_{XL,\text{rect}}(k)\right\} = \sigma^2_{XL}(k) + O_{\text{leak}}\left(N^{-1}\right)$$

with $X_0(k)$ the true DFT spectrum, O_{leak} the bias contribution of the noise leakage errors $T_{H_X}^{[p]}$ and $T_{H_L}^{[p]}$, and $\sigma^2_{XL}(k)$ the true noise (co-)variance

$$\sigma^2_{XL}(k) = \lambda_{XL}H_X(\Omega_k)\overline{H_L(\Omega_k)} \qquad (5)$$

$$\lambda_{XL} = E\left\{E_X^{[p]}(k)\overline{E_L^{[p]}(k)}\right\} = E\left\{e_x^{[p]}(t)e_l^{[p]}(t)\right\}$$

with $X, L \in \{U, Y\}$, $x, l \in \{u, y\}$, and $\lambda_{XX} = \lambda_X$. Finally, the sample means and the sample (co-)variances of the sample means of the input-output Fourier coefficients are given by

$$\hat{X}_{k,\text{rect}} = \frac{1}{\sqrt{N}}\hat{X}_{\text{rect}}(k) \qquad (6)$$

$$\hat{\sigma}^2_{k,\hat{X}\hat{L},\text{rect}} = \frac{1}{PN}\hat{\sigma}^2_{XL,\text{rect}}(k) \qquad (7)$$

where the factors $\frac{1}{P}$ and $\frac{1}{N}$ in (7) account for respectively the averaging over the P periods in (3), and the scaling in (6).

C. Nonparametric modeling - the overlap method

The overlap method [12] reduces the influence of the noise leakage errors in the DFT spectra by handling $P \geqslant 4$ periods of the input-output signals in blocks of 2 consecutive periods. To suppress the leakage at the excited DFT frequencies without introducing systematic errors, each block of two periods is multiplied by a time window of the type

$$w(t) = 1 + \alpha\cos(\pi t/N) + \beta\cos(3\pi t/N) \qquad (8)$$

$$w_{\text{rms}} = \text{rms}(w(t)) = \left(1 + 0.5\alpha^2 + 0.5\beta^2\right)^{1/2}$$

$$w_{\text{mean}} = \text{mean}(w(t)) = 1$$

for $t = 0, 1, \ldots, 2N - 1$, where N is the number of samples in one signal period, and with w_{rms} and w_{mean} respectively the rms and mean value of the window $w(t)$. To prove this statement it is sufficient to note that the DFT spectrum of the windowed signal

$$X_w^{[p]}(k) = \frac{1}{\sqrt{2N}w_{\text{rms}}}\sum_{t=0}^{2N-1} x^{[p]}(t)w(t)e^{-j\frac{2\pi kt}{2N}} \qquad (9)$$

with $p = 1, 2, \ldots, \frac{P}{2}$, evaluated at the even DFT lines $X_w^{[p]}(2k)$, is related to the unwindowed DFT spectrum $X^{[p]}(k)$ of 2 signal periods ((9) with $w(t) = 1$) as

$$w_{\text{rms}}X_w^{[p]}(k) = X^{[p]}(k) + \ldots$$
$$0.5\alpha\left(X^{[p]}(2k+1) + X^{[p]}(2k-1)\right) + \ldots$$
$$0.5\beta\left(X^{[p]}(2k+3) + X^{[p]}(2k-3)\right) \qquad (10)$$

where $X^{[p]}(k)$ contains no signal energy at the odd DFT lines (see Fig. 2). The choice $\alpha = -1$, $\beta = 0$ in (8) gives the Hanning window, while $\alpha = \beta = -\frac{1}{2}$ defines the minimum variance window [12]. The sample mean of the overlap method is the mean value of (9) over the $\frac{P}{2}$ blocks

$$\hat{X}_{\text{over}}(2k) = \frac{2}{P}\sum_{p=1}^{\frac{P}{2}} X_w^{[p]}(2k) \qquad (11)$$

Figure 2. DFT spectrum of $P = 2$ periods of a periodic signal (black arrows) disturbed by noise (gray arrows). Left noiseless, and right noisy signal.
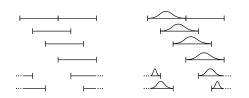

Figure 3. Circular overlap method with $r = 2/3\,\%$ overlap in blocks of two consecutive periods, without (left plot) and with (right plot) window.

where $X \in \{U, Y\}$.

To estimate the noise (co-)variances the following time domain residuals are first calculated

$$\hat{e}_x^{[p]}(t) = x^{[p]}(t) - \hat{x}(t) \qquad (12)$$

where $x^{[p]}(t)$ is the pth block of 2 consecutive signal periods, $p = 1, 2, \ldots, \frac{P}{2}$, and with $\hat{x}(t)$ the sample mean over the $\frac{P}{2}$ blocks. Next, the noise power spectra of the time domain residuals (12) are calculated via circular overlapping sub-records of length $2N$ (see Fig. (3), left plot). To suppress the leakage errors in the estimates, the sub-records are windowed with $w(t)$ (8) as shown in the right plot of Figure (3)

$$\hat{\sigma}_{XL,\,\text{over}}^2(2k) = \frac{1-r}{P} \sum_{i=1}^{\frac{P}{1-r}} \hat{E}_{X_W}^{[i]}(2k) \overline{\hat{E}_{L_W}^{[i]}(2k)} \qquad (13)$$

where $\hat{E}_{X_W}^{[i]}(k)$ is the DFT (9) of the windowed residual $\hat{e}_x^{[i]}(t)\, w(t)$ (12), and with r the fraction of overlap.

The expected values of the sample means (11) and the sample (co-)variances (13) equal

$$\begin{aligned}
E\left\{\hat{X}_{\text{over}}(2k)\right\} &= X_0(2k) \qquad (14) \\
E\left\{\hat{\sigma}_{XL,\,\text{over}}^2(2k)\right\} &= \sigma_{XL}^2(2k) + \ldots \\
& \quad O_{\text{leak}}\left(N_1^{-2}\right) + O_{\text{int}}\left(N_1^{-2}\right)
\end{aligned}$$

with $N_1 = 2N(1-r)$, $\sigma_{XL}^2(2k)$ the true (co-)variance defined in (5), and where O_{leak} and O_{int} are the bias contribution of respectively the noise leakage and the noise interpolation errors (proof: see [12]). The latter is due to the combination of 3 (Hanning window) or 5 (minimum variance window) noisy DFT lines in the windowed DFT spectrum (10). Finally, the sample means and the sample (co-)variances of the sample means of the input-output Fourier coefficients are given by

$$\hat{X}_{k,\,\text{over}} = \frac{w_{\text{rms}}}{\sqrt{2N}} \hat{X}_{\text{over}}(2k) \qquad (15)$$

$$\hat{\sigma}_{k,\,\hat{X}\hat{L},\,\text{over}}^2 = \frac{2}{P}\left(\frac{w_{\text{rms}}}{\sqrt{2N}}\right)^2 \hat{\sigma}_{XL,\,\text{over}}^2(2k) \qquad (16)$$

where $\frac{2}{P}$ and $\left(\frac{w_{\text{rms}}}{\sqrt{2N}}\right)^2$ in (16) accounts for respectively the averaging over the $\frac{P}{2}$ blocks in (11), and the scaling in (15). The factor w_{rms}^2 in (16) quantifies the increase in noise variance of the sample mean (11) w.r.t. that with a rectangular window: $w_{\text{rms}} = 1.225$ (or 1.76 dB) for the Hanning window; and $w_{\text{rms}} = 1.118$ (or 0.97 dB) for the minimum variance window.

D. Nonparametric modeling - the local polynomial approach

The local polynomial approach starts from the input-output DFT spectra of all measured data samples NP,

$$X(k) = \frac{1}{\sqrt{PN}} \sum_{t=0}^{PN-1} x(t)\, e^{-j\frac{2\pi kt}{PN}} \qquad (17)$$

where $P \geqslant 2$ and $X \in \{U, Y\}$. Next, the non-excited DFT lines (see, for example, the odd DFT frequencies in the right plot of Fig. 2) are used for estimating the noise (co-)variances and the noise transient terms. Finally, the input-output sample means are the DFT spectra at the excited frequencies minus the estimated noise transient terms. The whole procedure is explained in detail in the sequel of this section.

To calculate the input-output noise (co-)variances the input-output signals are put on top of each other into a 2×1 vector $z(t) = \begin{bmatrix} y(t) & u(t) \end{bmatrix}^T$, with x^T transpose of x. At the non-excited DFT frequencies $kP + m$, $k = 0, 1, \ldots, N/2 - 1$ and $m = 1, 2, \ldots, P - 1$, the DFT spectrum $Z(k)$ (17) of $z(t)$ only contains noise contributions of the form (2) that can be written as

$$\begin{aligned}
Z(kP+m) &= V(kP+m) + T_{H_Z}(\Omega_{kP+m}) \quad (18) \\
V(kP+m) &= H_Z(\Omega_{kP+m})\, E(kP+m)
\end{aligned}$$

where $T_{H_Z}(\Omega)$ is a smooth function of the frequency. Following the lines of [6] $T_{H_Z}(\Omega_{kP+m})$ is be expanded at the excited frequency $\Omega = \Omega_{kP}$ using Taylor's formula with remainder

$$\begin{aligned}
T_{H_Z}(\Omega_{kP+m}) &= T_{H_Z}(\Omega_{kP}) + \sum_{r=1}^{R} t_r(k)\, m^r + \ldots \\
& \quad (PN)^{-1/2} O\left(N_2^{-(R+1)}\right) \qquad (19)
\end{aligned}$$

with $N_2 = \frac{PN}{m}$. The $O()$ term in the remainder stems from the frequency difference $f_{kP+m} - f_{kP} = \frac{m}{PN} f_s$, and the additional factor $(PN)^{-1/2}$ in the remainder originates from the fact that $T_{H_Z}(\Omega)$ is an $O\left(N^{-1/2}\right)$ [3]. Neglecting the remainder in (19), (18) can be written as

$$Z(kP+m) = \Theta K(m) + V(kP+m) \qquad (20)$$

where Θ is the $2 \times (R+1)$ complex matrix of the unknown transient parameters

$$\Theta = \begin{bmatrix} T_{H_Z}(\Omega_{kP}) & t_1(k) & t_2(k) & \dots & t_R(k) \end{bmatrix} \quad (21)$$

$K(m)$ is the $(R+1) \times 1$ vector containing the powers of m

$$K(m) = \begin{bmatrix} 1 & m & \dots & m^R \end{bmatrix}^T \quad (22)$$

Collecting (20) for $2n$ consecutive non-excited DFT lines $kP \pm m_i$, with m_i, $i = 1, 2, \dots, n$, the first n numbers of the set $\mathbb{N} \setminus \{kP \mid k \in \mathbb{N}\}$, gives

$$Z_n = \Theta K_n + V_n \quad (23)$$

where Z_n, K_n, and V_n are respectively $2 \times 2n$, $(R+1) \times 2n$, and $2 \times 2n$ matrices of the form

$$X_n = \begin{bmatrix} X(kP - m_n) & \dots & X(kP - m_1), \\ X(kP + m_1) & \dots & X(kP + m_n) \end{bmatrix} \quad (24)$$

with $X = Y$, K, and V. Note that (23) does not contain the DFT frequency kP of the Taylor series expansion (19). This is the main difference with the approach in [6].

Choosing $2n > R+1$, (23) is an overdetermined set of equations in the unknown transient parameters Θ that can be solved in least squares sense as

$$\hat{\Theta} = Z_n K_n^H \left(K_n K_n^H \right)^{-1} = Z_n U_1 \Sigma_1^{-1} V_1^H \quad (25)$$

with $U_1 \Sigma_1 V_1^H$ the singular value decomposition of K_n^H, and where x^H is the hermitian (complex conjugate) transpose of x. The residual of the least squares fit $\hat{V}_n = Z_n - \hat{\Theta} K_n$ is related to the noise V_n as,

$$\begin{aligned} \hat{V}_n &= V_n P_n \\ P_n &= I_{2n} - K_n^H \left(K_n K_n^H \right)^{-1} K_n \end{aligned} \quad (26)$$

where the idempotent matrix P_n has rank $2n - (R+1)$. Assuming that the noise is white in the band $[kP - m_n, kP + m_n]$, an estimate of the noise covariance matrix $C_V(kP) = \text{Cov}(V(kP))$ at the excited DFT frequency kP, with $V(kP)$ defined in (18), is obtained as

$$\hat{C}_V(kP) = \frac{1}{q} \hat{V}_n \hat{V}_n^H \quad (27)$$

with $q = 2n - (R+1)$. Eq. (27) defines the local polynomial estimates of the input-output noise (co-)variances

$$\begin{aligned} \hat{\sigma}_{Y,\text{ poly}}^2(kP) &= \left(\hat{C}_V(kP) \right)_{[1,1]} \\ \hat{\sigma}_{U,\text{ poly}}^2(kP) &= \left(\hat{C}_V(kP) \right)_{[2,2]} \\ \hat{\sigma}_{YU,\text{ poly}}^2(kP) &= \left(\hat{C}_V(kP) \right)_{[1,2]} \end{aligned} \quad (28)$$

Recalling that the first column of $\hat{\Theta}$ is an estimate of the input and output noise transient terms,

$$\hat{\Theta}_{[:,1]} = \hat{T}_{H_Z}(\Omega_{kP}) = \begin{bmatrix} \hat{T}_{H_Y}(\Omega_{kP}) \\ \hat{T}_{H_U}(\Omega_{kP}) \end{bmatrix} \quad (29)$$

with $X_{[:,1]}$ the first column of X, the local polynomial estimates of the input-output sample means are calculated as

$$\begin{aligned} \hat{Y}_{\text{poly}}(kP) &= Y(kP) - \hat{T}_{H_Y}(\Omega_{kP}) \\ \hat{U}_{\text{poly}}(kP) &= U(kP) - \hat{T}_{H_U}(\Omega_{kP}) \end{aligned} \quad (30)$$

The expected value of the sample means (30) and sample (co-)variances (25) equal

$$\begin{aligned} E\left\{ \hat{X}_{\text{poly}}(kP) \right\} &= X_0(kP) \quad (31) \\ E\left\{ \hat{\sigma}_{XL,\text{ poly}}^2(kP) \right\} &= \sigma_{XL}^2(kP) + \dots \\ & O_{\text{leak}}\left(N_3^{-(R+2)} \right) + O_{\text{int}}\left(N_3^{-2} \right) \end{aligned}$$

with $N_3 = PN/m_n$, $\sigma_{XL}^2(2k)$ the true (co-)variance defined in (5), and where O_{leak} and O_{int} are the bias contribution of respectively the noise leakage and the noise interpolation errors. The latter is due to the combination of $2n$ noisy DFT lines in the linear least squares estimate (25). Finally, the sample means and the sample (co-)variances of the sample means of the input-output Fourier coefficients are given by

$$\hat{X}_{k,\text{ poly}} = \frac{1}{\sqrt{PN}} \hat{X}_{\text{poly}}(kP) \quad (32)$$

$$\hat{\sigma}_{k,\hat{X}\hat{L},\text{ poly}}^2 = \mu_{\text{poly}} \frac{1}{PN} \hat{\sigma}_{XL,\text{ poly}}^2(kP) \quad (33)$$

where $\frac{1}{PN}$ in (33) accounts for the scaling in (32). The factor μ_{poly} quantifies the increase in noise variance of the sample means (30) w.r.t. the DFT spectra $X(kP)$ without leakage (transient) suppression, and is calculated as

$$\mu_{\text{poly}} = 1 + \left\| \Sigma_1^{-1} V_{1[1,:]}^H \right\|_2^2 \quad (34)$$

with $\|x\|_2^2 = x^H x$, $X_{[1,:]}$ the first row of X, and Σ_1, V_1 defined in (25). Numerous simulations indicate that the variance increase due to the leakage suppression μ_{poly} is about 1 dB.

E. Comparison of the methods

The expected value of the estimated Fourier coefficients (6), (15), and (32), and their estimated (co-)variances (7), (16), and (33), can be written as

$$E\left\{ \hat{X}_{k,\text{ estim}} \right\} = X_{k,0} \quad (35)$$

$$E\left\{ PN \hat{\sigma}_{k,\hat{X}\hat{L},\text{ estim}}^2 \right\} = \mu_{\text{estim}} \sigma_{XL}^2(k) + b_{\text{estim}} \quad (36)$$

with estim $\in \{\text{rect, over, poly}\}$, $\sigma_{XL}^2(k)$ the true noise (co-)variance defined in (5), $X_{k,0}$ the true Fourier coefficient,

$\mu_{\text{rect}} = 0\,\text{dB}$, $\mu_{\text{over}} = 0.97\,\text{dB}$ for the minimum variance window, and $\mu_{\text{poly}} \approx 1\,\text{dB}$. The bias term b_{estim} in (36) decreases to zero for $N \to \infty$ as $b_{\text{rect}} = O\left(N^{-1}\right)$ for the classical method, $b_{\text{over}} = O\left(N^{-2}\right)$ for the overlap method, and $b_{\text{poly}} = O\left((PN)^{-2}\right)$ for the local polynomial approach.

The following conclusions can be made. In those frequency bands where the noise leakage (transient) terms in (2) are dominant, we have that $b_{\text{estim}} > \mu_{\text{estim}}\sigma_{XL}^2\,(k)$ in (36). Hence,

$$\hat{\sigma}_{k,\,\hat{X}\hat{L},\,\text{poly}}^2 < \hat{\sigma}_{k,\,\hat{X}\hat{L},\,\text{over}}^2 \ll \hat{\sigma}_{k,\,\hat{X}\hat{L},\,\text{rect}}^2 \tag{37}$$

because the local polynomial approach and the classical method have respectively the best and the worst leakage suppression properties. However, if the noise transient terms can be neglected, then $b_{\text{estim}} < \mu_{\text{estim}}\sigma_{XL}^2\,(k)$, and

$$\hat{\sigma}_{k,\,\hat{X}\hat{L},\text{poly}}^2 \approx \hat{\sigma}_{k,\,\hat{X}\hat{L},\,\text{over}}^2 = 1.25\hat{\sigma}_{k,\,\hat{X}\hat{L},\,\text{rect}}^2 \tag{38}$$

The factor 1.25 (about 1 dB) in (38) is the (small) price to be paid for estimating and removing a zero leakage contribution in the sample means.

F. Non-steady state conditions

If the input-output signals in Figure 1 are measured under non-steady state conditions, then (1) is replaced by

$$X^{[p]}(k) = X_0(k) + N_X^{[p]}(k) + T_{G_X}^{[p]}(\Omega_k) \tag{39}$$

where the input-output transient terms $T_{G_X}(\Omega)$, $X = U, Y$, are rational functions that depend on the dynamics of the actuator, the system, and the controller, and on the difference between the initial and final conditions of the experiment [3]. Combining (2) and (39) it follows that no distinction can be made between the input-output noise transient (leakage) terms and the input-output system transients, and that (18), where T_{H_Z} is replaced by $T_Z = T_{H_Z} + T_{G_Z}$, remains valid. As a consequence, the overlap (Section II-C) and local polynomial (Section II-D) methods also suppress the system transients and, therefore, can also be applied to non-steady state measurements. For lowly damped systems this may result in a significant reduction of the experiment time. Since the local polynomial approach supresses much better the transient (leakage) errors than the overlap method (compare O_{leak} in eq. (14) and (31)), it can be concluded that the local polynomial approach is (much) less sensitive to the system transients in the measurements.

III. NONPARAMETRIC FRF MODELING

A nonparametric estimate of the frequency response function (FRF) is obtained by dividing the estimated input-output Fourier coefficients (6), (15), (32)

$$\hat{G}_{\text{estim}}(\Omega_k) = \hat{Y}_{k,\,\text{estim}}/\hat{U}_{k,\,\text{estim}} \tag{40}$$

For noisy input observations the FRF estimate (40) is biased. However, if the input signal-to-noise ratio $\left|\hat{U}_{k,\,\text{estim}}\right|/\hat{\sigma}_{k,\,\hat{U},\,\text{estim}}$ is larger than 10 dB, then the relative bias
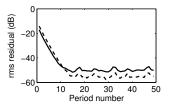

Figure 4. Root mean square (rms) value of the difference between each signal period and the last signal period (dashed line: input signal; solid line: output signal).

on the FRF estimate is smaller than 10^{-4} [3]. Although the variance of the FRF estimate (40) does not exist, confidence bounds with a given confidence level can be constructed using the following variance expression [3], [4]

$$\hat{\sigma}_{\hat{G}}^2(k) = \left|\hat{G}(\Omega_k)\right|^2 \left(\frac{\hat{\sigma}_{\hat{Y}_k}^2}{\left|\hat{Y}_k\right|^2} + \frac{\hat{\sigma}_{\hat{U}_k}^2}{\left|\hat{U}_k\right|^2} - 2\text{Re}\left(\frac{\hat{\sigma}_{\hat{Y}_k\hat{U}_k}^2}{\hat{Y}_k\hat{U}_k}\right)\right)$$

with $\text{Re}(x)$ the real part of x, and where $\hat{\sigma}_{\hat{X}_k\hat{L}_k}^2$, $X, L \in \{Y, U\}$, denotes the noise (co-)variance $\hat{\sigma}_{k,\,\hat{X}\hat{L},\,\text{estim}}^{2,\,\text{noise}}$.

IV. EXAMPLE: FLEXURAL VIBRATIONS OF A STEEL BEAM

A steel beam (density 7800 kg/m^3, length 61 cm, height 2.47 cm, and width 4.93 mm) under free-free boundary conditions is excited in its transverse direction by a periodic force applied at 10 cm from the end of the beam (see [11] for a detailed description of the experimental set up). The force (excitation) and acceleration (response) at the excitation point are measured with an impedance head. The generator and acquisition units all operate at the same sampling frequency $f_s = 10\,\text{MHz}/2^9 \approx 19.531\,\text{kHz}$. A crest factor optimized multisine excitation $r(t)$ [3] consisting of the sum of $F = 306$ harmonically related frequencies kf_s/N ($k = 1, 2, \ldots, F$, and $N = 1024$) in the band (0 Hz, 6 kHz], with equal harmonic amplitudes, is applied to the steel beam via a mini-shaker. The rms-value of the resulting force signal $u(t)$ equals 99 mV, and the first 50 periods of the force $u(t)$ and acceleration $y(t)$ signals are measured. Subtracting the last signal period from the other signal periods and calculating the rms value of the residuals over each period, it follows (see Figure 4) that the system reaches steady state (the system transients are below the noise level) after about 14 periods. Therefore, the last $P = 36$ measured periods are used for the analysis under steady state conditions.

The sample means and sample (co-)variances of the Fourier coefficients are calculated using the classical (rectangular window) method (7), the overlap method with $r = 3/4$ (15), (16), and the local polynomial approach (32), (33) with $R = 2$ (second order polynomial approximation). For the local polynomial approach, n in (27) is chosen such that the equivalent number of degrees of freedom (dof) $q = 2n - (R + 1)$ of the noise variance estimate is the same as that of the classical approach where dof $= P - 1 = 35$. For the 75% overlap
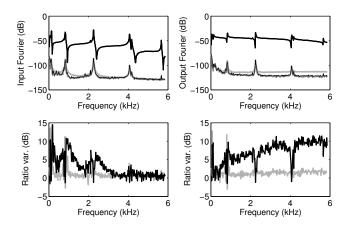
Figure 5. Estimated input-output Fourier coefficients and their variance of the steady state measurements (last 36 periods)- steel beam. Top row: DFT spectra (bold black), variance rectangular window (light gray), variance overlap (thin black), and variance local polynomial approach (dark gray). Bottom row: ratio var$_{rect}$/var$_{poly}$ (bold black); and var$_{overlap}$/var$_{poly}$ (light gray).
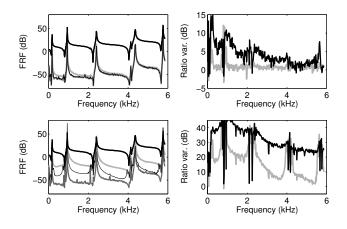

Figure 6. Estimated FRF estimated and its variance - steel beam. Top row: steady state measurements (last 36 periods). Bottom row: transient measurements (first 36 periods). Left column: FRF (bold black); variance rectangular window (light gray); variance overlap (thin black); and variance local polynomial approach (dark gray). Right column: ratio var$_{rect}$/var$_{poly}$ (bold black); and var$_{overlap}$/var$_{poly}$ (light gray).

method the equivalent number of degrees of freedom equals dof $= 27$.

Figure 5 shows the estimated input-output Fourier coefficients and the top row of Figure 6 the corresponding FRF estimates. It can be seen that the noise variance of the rectangular window estimates is almost everywhere significantly larger than that of the overlap method and the local polynomial approach. Note also that the noise variance of the overlap estimates is at least 0.5 dB larger than that of the local polynomial approach (see the light gray lines of Figure 5, bottom row, and Figure 6, bottom right plot). Both observations indicate that the noise leakage is important this experiment. It can be explained by the lowly damped resonances in the input-output noise power spectra (see the bold black lines of Figure 5, top row).

To verify the robustness of the methods w.r.t. system transients, the same calculations are repeated on the first $P = 36$ measured periods. The results are shown in Figure 6. It can be seen that the variance of the overlap and the rectangular window FRF estimates using the transient measurements (bottom row) are much larger than those using the steady state measurements (top row). This is not the case for the local polynomial FRF estimates: except at a few frequencies, the variance using the transient data almost coincides (only 0.5 dB larger) with the variance using the steady state measurements. We conclude that the local polynomial approach is much more robust to system transients than the classical methods.

V. CONCLUSIONS

A nonparametric method for estimating the frequency response function and its noise variance from noisy input-output observations of dynamic systems excited by periodic signals has been presented. The only assumption made is that the noise dynamics is a smooth function of the frequency that can locally be approximated very well by a polynomial of degree R. A theoretical analysis confirmed by a real life experiment shows

that the local polynomial approach with $R \geq 2$ suppresses much better the noise transients than the classical methods. Moreover, the local polynomial approach is robust to the presence of system transients. Hence, measuring the first two periods of the transient response to a periodic input is enough for the local polynomial approach. For lightly damped systems this implies a significant reduction in measurement time.

REFERENCES

[1] J. S. Bendat, and A. G. Piersol, *Engineering Applications of Correlations and Spectral Analysis.* New York (USA):Wiley, 1980.

[2] D. R. Brillinger, *Time Series: Data Analysis and Theory.* New York (USA): McGraw-Hill, 1981.

[3] R. Pintelon, and J. Schoukens, *System Identification: A Frequency Domain Approach.* Piscataway (USA): IEEE Press, 2001.

[4] W. P. Heath, "The variance of nonparametric errors-in-variables estimates," *IEEE Trans. Instr. and Meas.*, vol. 54, no. 1, pp. 228-236, 2005.

[5] T. Schultz, M. Sheplak, L.N. Cattafesta, "Application of multivariate uncertainty analysis to frequency response function estimates," *Journ. Sound and Vibr.*, vol. 305, no. 1-2, pp. 116-133, 2007.

[6] J. Schoukens, Y. Rolain, and R. Pintelon, "Leakage reduction in frequency response function measurements," *IEEE Trans. Instr. and Meas.*, vol. 55, no. 6, pp. 2286-2291, 2006.

[7] J. Antoni, and J. Schoukens, "A comprehensive study of the bias and variance of frequency-response-function measurements: optimal window selection and overlapping strategies," *Automatica*, vol. 43, no. 10, pp. 1723-1736, 2007.

[8] K. Barbé, J. Schoukens, and R. Pintelon, "Frequency domain errors-in-variables estimation of linear dynamic systems using data from overlapping sub-records," *IEEE Trans. Instr. and Meas.*, vol. 57, no. 8, pp. 1529-1536, 2008.

[9] J. Schoukens, and R. Pintelon, "Estimation of nonparametric noise models for linear dynamic systems," *IEEE Trans. Instr. and Meas.*, vol. 58, no. 8, pp. 2468-2474, 2009.

[10] T. D'haene, R. Pintelon, J. Schoukens, and E. Van Gheem, "Variance analysis of frequency response function measurements using periodic excitations," *IEEE Trans. Instr. and Meas.*, vol. 54, no. 4, pp. 1452-1456, 2005.

[11] R. Pintelon, P. Guillaume, S. Vanlanduit, K. De Belder and Y. Rolain, "Identification of Young's modulus from broadband modal analysis experiments," *Mech. Sys. & Sign. Proc.*, vol. 18, no. 4, pp. 699-726, 2004.

[12] K. Barbé, *Identification and Use of Nonparametric Noise Models from Overlapping Subrecords*, PhD thesis, Vrije Universiteit Brussel, dept. ELEC, Pleinlaan 2, 1050 Brussel (Belgium), 2009.